Tuning of Charge Density Wave Strengths by Competition between Electron−Phonon Interaction of $Pd^{II}-Pd^{IV}$ Mixed-Valence States and Electron Correlation of Ni^{III} States in Quasi-One-Dimensional Bromo-Bridged Ni−Pd Mixed-Metal MX Chain Compounds $Ni_{1-x}Pd_x(chxn)_2Br_3$

Masahiro Yamashita,*,† Tomohiko Ishii,† Hiroyuki Matsuzaka,† Toshio Manabe,‡ Takuya Kawashima,‡ Hiroshi Okamoto,§ Hiroshi Kitagawa,|| Tadaoki Mitani,|| Kazuhiro Marumoto,⊥ and Shin-ichi Kuroda⊥

Graduate School of Science & PRESTO (JST), Tokyo Metropolitan University, 1-1 Minamiohsawa, Hachioji, Tokyo 192-0397, Japan, Graduate School of Human Informatics, Nagoya University, Chikusa-ku, Nagoya 464-8601, Japan, Department of Applied Physics & PRESTO (JST), The University of Tokyo, Hongo, Bunkyo-ku, Tokyo 113-8656, Japan, Japan Advanced Institute for Science and Technology, Ishikawa 923-1292, Japan, and Department of Applied Physics, Nagoya University, Chikusa-ku, Nagoya 464-8603, Japan

Received February 23, 1999

A series of single crystals of quasi-one-dimensional bromo-bridged Ni−Pd mixed-metal MX chain compounds $Ni_{1-x}Pd_x(chxn)_2Br_3$ (chxn = 1(*R*),2(*R*)-diaminocyclohexane) have been obtained by electrochemical oxidation methods of the mixed methanol solutions of parent Ni^{II} complex $[Ni(chxn)_2]Br_2$ and Pd^{II} complex $[Pd(chxn)_2]Br_2$ with various mixing ratios. To investigate the competition between the electron correlation of the Ni^{III} states (or spin density wave states) and the electron−phonon interaction of the $Pd^{II}-Pd^{IV}$ mixed-valence states (or charge density wave states) in the Ni−Pd mixed-metal compounds, IR, Raman, ESR, XP, and Auger spectra have been measured. The IR, resonance Raman, XP, and Auger spectra show that the $Pd^{II}-Pd^{IV}$ mixed-valence states are influenced and gradually approach the Pd^{III} states with the increase of the Ni^{III} components. This means that in these compounds the electron−phonon interaction in the $Pd^{II}-Pd^{IV}$ mixed-valence states is weakened with the strong electron correlation in the Ni^{III} states.

Introduction

Recently low-dimensional compounds have attracted much attention because they show very interesting physical properties such as Peierls transition, spin-Peierls transition, neutral−ionic transition, charge density wave (CDW) states, spin density wave (SDW) states, superconductivities, etc.[1] Among these compounds, quasi-one-dimensional halogen-bridged mixed-valence compounds (hereafter abbreviated as MX chains) have been extensively investigated during the last 20 years, because of their interesting physical properties such as intense and dichroic intervalence charge-transfer bands, progression of overtones of resonance Raman spectra, luminescences with large Stokes shifts, midgap absorptions attributable to solitons and polarons,

† Tokyo Metropolitan University.
‡ Graduate School of Human Informatics, Nagoya University.
§ The University of Tokyo.
|| Japan Advanced Institute for Science and Technology.
⊥ Department of Applied Physics, Nagoya University.

(1) (a) *Extended Linear Chain Compounds*; Miller, J. S., Ed.; Plenum: New York and London, 1982; Vols. I−III. (b) Robin, M. B.; Day, P. *Adv. Inorg. Radiochem.* **1967**, *10*, 247. (c) Interrante, L. V.; Browall, K. W. *Inorg. Chem.* **1974**, *13*, 5.

(2) (a) Yamashita, M. In *New Functional Materials, Volume C, Synthetic Process and Control of Functionality Materials*; Tsuruta, T., Doyama, M., Seno, M., Eds.; Elsevier Science Publisher: Tokyo, 1993; p 539. (b) Bishop, A. R.; Swanson, B. I. *Los Alamos Sci.* **1993**, *21*, 133. (c) Clark, R. J. H. *Adv. Infrared Raman Spectrosc.* **1983**, *11*, 95. (d) Okamoto, H.; Yamashita, M. *Bull. Chem. Soc. Jpn.* **1998**, *71*, 2023. (e) Clark, R. J. H. *Chem. Soc. Rev.* **1990**, *19*, 107. (f) Papavassiliou, G. C.; Zdetsis, A. D. *J. Chem. Soc., Faraday Trans. 2* **1980**, *76*, 104. (g) Papavassiliou, G. C.; Jacobsen, C. S. *J. Chem. Soc., Faraday Trans. 2* **1981**, *77*, 191. (h) Yamashita, M.; Manabe, T.; Inoue, K.; Kawashima, T.; Okamoto, H.; Kitagawa, H.; Mitani, T.; Toriumi, K.; Miyamae, H.; Ikeda, R. *Inorg. Chem.* **1999**, *38*, 1894. (i) Yamashita, M.; Miya, S.; Kawashima, T.; Manabe, T.; Sonoyama, T.; Kitagawa, H.; Mitani, T.; Okamoto, H.; Ikeda, R. *J. Am. Chem. Soc.* **1999**, *121*, 2321.

(3) (a) Wada, Y.; Era, K.; Yamashita, M. *Solid State Commun.* **1988**, *67*, 953. (b) Ooi, H.; Yamashita, M.; Kobayashi, T. *Solid State Commun.* **1993**, *86*, 789. (c) Ooi, H.; Yamashita, M.; Kobayashi, T. *Chem. Phys. Lett.* **1993**, *210*, 384. (d) Wada, Y.; Lemmer, U.; Gobel, E. O.; Yamashita, M. *J. Luminesc.* **1994**, *58*, 146. (e) Wada, Y.; Lemmer, U.; Gobel, E. O.; Yamashita, M.; Toriumi, K. *Phys. Rev. B* **1995**, *52*, 8276. (f) Kobayashi, T.; Sekikawa, T. Yamashita, M. *Chem. Lett.* **1997**, 1029.

(4) (a) Donohoe, R. J.; Worl, L. A.; Arrington, C. A.; Bulou, A.; Swanson, B. I. *Phys. Rev. B* **1992**, *45*, 1992. (b) Matsushita, N.; Kojima, N.; Ban, T.; Tsujikawa, I. *J. Phys. Soc. Jpn.* **1987**, *19*, 907. (c) Kuroda, N.; Sakai, M.; Nishina, Y.; Tanaka, M.; Kurita, S. *Phys. Rev. Lett.* **1987**, *58*, 2122. (d) Okamoto, H.; Mitani, T.; Toriumi, K.; Yamashita, M. *Phys. Rev. Lett.* **1992**, *69*, 2248. (e) Okamoto, H.; Oka, Y.; Mitani, T.; Toriumi, K.; Yamashita, M. *Mol. Cryst. Liq. Cryst.* **1994**, *256*, 161. (f) Wada, Y.; Matsushita, N.; Yamashita, M. *Mol. Cryst. Liq. Cryst.* **1994**, *256*, 891. (g) Okamoto, H.; Shimada, Y.; Kagami, Y.; Oka, Y.; Yamashita, M.; Manabe, T.; Mitani, T. *Synth. Met.* **1997**, *86*, 1803. (h) Okamoto, H.; Oka, Y.; Mitani, T.; Yamashita, M. *Phys. Rev. B* **1997**, *55*, 6330. (i) Huang, X. Z.; Saxena, A.; Bishop, A. R.; Worl, L. A.; Love, S. P.; Swanson, B. I. *Solid State Commun.* **1992**, *84*, 957. (j) Worl, L. A.; Huckett, S. C.; Swanson, B. I.; Saxena, A.; Bishop, A. R.; Gammel, J. T. *J. Phys.: Condens. Matter* **1992**, *4*, 10237. (k) Bardeau, J.-F.; Bulou, A.; Swanson, B. I. *J. Raman Spectrosc.* **1995**, *26*, 1051. (l) Scott, B. Bracewell, B. L.; Johnson, S. R.; Swanson, B. I.; Bardeau, J.-F.; Bulou, A. Chem. Mater. **1996**, *8*, 321.

10.1021/ic990219i CCC: $18.00
Published on Web 10/14/1999

large third-order nonlinear optical properties, one-dimensional model compounds of high T_c copper oxide superconductors, etc.[2] The excited states and their relaxation process have been investigated as a prototype material of one-dimensional electron−phonon systems by using the pico- and femtosecond time-resolved optical methods.[3] The creations of the solitons and polarons were found to be controlled by using the difference of the dimensionalities of CDW states.[4] The third-order nonlinear optical susceptibilities of the compounds are almost equal to that of polydiacetylene.[5]

From the theoretical viewpoints,[6] the MX chains are considered as a Peierls−Hubbard system where the electron−phonon interaction (*S*), the electron-transfer energy (*T*), the on-site and intersite Coulomb interactions (*U* and *V*, respectively) compete or cooperate with one another. Originally, these MX chains are considered as a one-dimensional metallic state with the half-filled d_{z^2} orbital of metals and the filled p_z orbitals of bridging halogens. However, as it is well-known, the one-dimensional metallic state is unstable and subsequently transferred to the insulating state by the electron−phonon interaction (*S*) and the electron correlation (*U*). In most MX chains, due to the strong electron−phonon interaction, the bridging halogens are distorted from the midpoints between the neighboring two metal atoms, giving CDW states or $M^{II}-M^{IV}$ mixed-valence states ($\cdots M^{II}\cdots X-M^{IV}-X\cdots M^{II}\cdots$). Accordingly, the half-filled metallic band is split into the occupied valence band and the unoccupied conduction band with finite Peierls gaps. Therefore, these compounds belong to the class II type of the Robin−Day classification for the mixed-valence complexes.[1b] These compounds are formulated as $[M^{II}(AA)_2][M^{IV}(AA)_2X_2]Y_4$ ($M^{II}-M^{IV}$ = $Pt^{II}-Pt^{IV}$, $Pd^{II}-Pd^{IV}$, $Ni^{II}-Pt^{IV}$, $Pd^{II}-Pt^{IV}$, $Cu^{II}-Pt^{IV}$; X = Cl, Br, I, and mixed halides; AA = ethylenediamine (en), cyclohexanediamine (chxn), etc.; Y = ClO_4, BF_4, X, etc.). These MX chains have two characteristic points compared with the inorganic semiconductors and organic conjugated polymer as follows: The magnitudes of the band gaps or CDW strengths can be tuned by varying chemical factors such as M, X, AA, and Y; in other words, the physical parameters (*S*, *T*, *U*, and *V*) can be tuned by substitution of the chemical factors. Moreover, the interchain interaction can be controlled by using the intra- and interchain hydrogen bond networks between amino hydrogens and counteranions.[7]

On the other hand, theoretically it was proposed that in the case of stronger on-site Coulomb interaction (*U*) compared with the electron−phonon interaction (*S*), the M^{III} state or SDW state is considered to be more stable, where the bridging halogens are located at the midpoints between two neighboring metal atoms ($-X-M^{III}-X-M^{III}-X-$). Recently, our groups have succeeded in synthesizing such compounds formulated as $[Ni^{III}(chxn)_2X]X_2$ (chxn = 1(*R*),2(*R*)-diaminocyclohexane; X = Cl, Br, and mixed halides; Y = Cl, Br, mixed halides, ClO_4, BF_4, and NO_3),[2h] since a Ni ion has stronger *U* compared with that of a Pd or Pt ion and/or compared with *S* in a Ni ion. These Ni compounds show very strong antiferromagnetic interaction among spins located on the $3d_{z^2}$ orbital in each Ni ion through the bridging halogens. These compounds belong to the class III type of the Robin−Day classification for the mixed-valence complexes.[1b] The XP, Auger, and single-crystal reflectance spectra have revealed that these Ni compounds are not Mott insulators but charge-transfer insulators, where the energy levels of the bridging halogens are located between the upper and lower Hubbard bands. Therefore, the electronic structures of the Ni compounds are similar to those of the starting materials of copper oxide superconductors except for their dimensionality.[8]

The $[Ni(chxn)_2Br]Br_2$ and $[Pd(chxn)_2][Pd(chxn)_2Br_2]Br_4$ (hereafter abbreviated as $Pd(chxn)_2Br_3$) are isomorphous with each other (same space group, *I*222), although the positions of the bridging halogens are different from each other, that is, located at midpoints and distorted from the midpoints between two neighboring metal ions, respectively. If we can obtain the single crystals of the Ni−Pd mixed-metal compounds, directly we can investigate the competition between the electron correlation of the Ni^{III} states (SDW states) and the electron−phonon interaction of the $Pd^{II}-Pd^{IV}$ mixed-valence states (CDW states) in this system. As to the studies on the transition metal oxides, the filling control or doping method is usually employed, where the physical parameters are controlled indirectly. On the other hand, in MX chain compounds, we can control the physical parameters (*S*, *T*, *U*, and *V*) directly by substituting the chemical factors such as metal ions, bridging halogens, etc.

According to such a strategy, we have synthesized and investigated the physical properties of a series of $Ni_{1-x}Pd_x(chxn)_2Br_3$ compounds with various mixing ratios.

Experimental Section

A series of single crystals of the Ni−Pd mixed-metal compounds $Ni_{1-x}Pd_x(chxn)_2Br_3$ were obtained by the electrochemical oxidation method of the mixed methanol solutions of $[Ni(chxn)_2]Br_2$ and $[Pd(chxn)_2]Br_2$ with various mixing ratios at room temperature using H-shaped cells. Current dependence and concentration dependence were investigated. As electrolyte, tetra-*n*-butylammonium bromide was used. The elemental analyses of Ni and Pd were carried out by ICP emission spectrometry on a SEIKO SPS 7000 plasma spectrometer.[9] Generally, the ratios of the Pd/Ni ions were found to increase a little more in solids compared with those in solutions.

For IR absorption measurements, powder samples ground down from single crystals were diluted with KBr, and then the mixtures were processed into pellets under pressure (~6 kbar). IR spectra were measured in the temperature range of 11−300 K by a Nicolet FTIR 800 spectrometer with a DAIKIN CryoKelvin cryostat that possesses KRS-5 optical windows. IR detectors of TGS and MCT were used.

Crystal parameters (*a*, *b*, and *c* axes) were measured on a MAC Science MPX3 using Mo Kα radiation at room temperature.

Raman spectra were measured for single crystals with Ar^+ excitation using a JASCO NR-1800 laser Raman spectrometer. A Spectra-Physics model 2017 Ar^+ laser provided the exciting line (514.5 nm). Detection

(5) Iwasa, Y.; Funatsu, E.; Koda, T.; Yamashita, M. *Mol. Cryst. Liq. Cryst.* **1992**, *217*, 37.
(6) (a) Nasu, K. *J. Phys. Soc. Jpn*. **1983**, *52*, 3865. (b) Nasu, K. *J. Phys. Soc. Jpn*. **1984**, *53*, 302. (c) Nasu, K. *J. Phys. Soc. Jpn*. **1984**, *53*, 427. (d) Gammel, G. T.; Saxena, A.; Batistic, I.; Bishop, A. R.; Phillpot, S. R. *Phys. Rev. B* **1992**, *45*, 6408. (e) Nasu, K. *Physica* **1986**, *143B*, 229. (f) Maruo T. *Physica* **1986**, *143B*, 273. (f) Huang, X. Z.; Bishop, A. R. *Phys. Rev. B* **1993**, *48*, 16148. (g) Kuroda, N.; Kataoka, M.; Nishina, Y. *Phys. Rev. B.* **1991**, *44*, 13260.
(7) (a) Okamoto, H.; Mitani, T.; Toriumi, K.; Yamashita, Y. *Mater. Sci. Eng*. **1992**, *B13*, 9. (b) Huckett, S. C.; Scott, B.; Love, A. P.; Donohoe, R. J.; Burns, C. J.; Garcia, E.; Frankvom, T.; Swanson, B. I. *Inorg. Chem*. **1993**, *32*, 2137. (c) Larsen, K. P.; Toftlund, H. *Acta Chem. Scand.* **1977**, *31*, 182.
(8) (a) Toriumi, K.; Wada, Y.; Mitani, T.; Bandow, S.; Yamashita, M.; Fujii, Y. *J. Am. Chem. Soc*. **1989**, *111*, 2341. (b) Toriumi, K.; Okamoto, H.; Mitani, T.; Bandow, S.; Yamashita, M.; Wada, Y.; Fujii, Y.; Clark, R. J. H.; Michael, D. J.; Edward, A. J.; Watkin, D.; Kurmoo, M.; Day, P. *Mol. Cryst. Liq. Cryst.* **1990**, *181*, 333. (c) Okamoto, H.; Toriumi, K.; Mitani, T.; Yamashita, M. *Phys. Rev. B* **1990**, *42*, 10381. (d) Okamoto, H.; Shimada, Y.; Oka, Y.; Chainani, A.; Takahashi, T.; Kitagawa, H.; Mitani, T.; Toriumi, K.; Manabe, T.; Yamashita, M. *Phys. Rev. B* **1996**, *54*, 8438.
(9) (a) Manabe, T.; Kawashima, T.; Yamashita, M.; Okamoto, H.; Kitagawa, H.; Mitani, T.; Inokuchi, M.; Yakushi, K. *Synth. Met*. **1997**, *86*, 2233. (b) Manabe, T.; M. Yamashita, M.; Kawashima, T.; Okamoto, H. Kitagawa, H.; Mitani, T.; Miyamae, H.; Inoue, K.; Yakushi, K. *Opt. Probes Conjugated Polym*. **1997**, *3145*, 106.

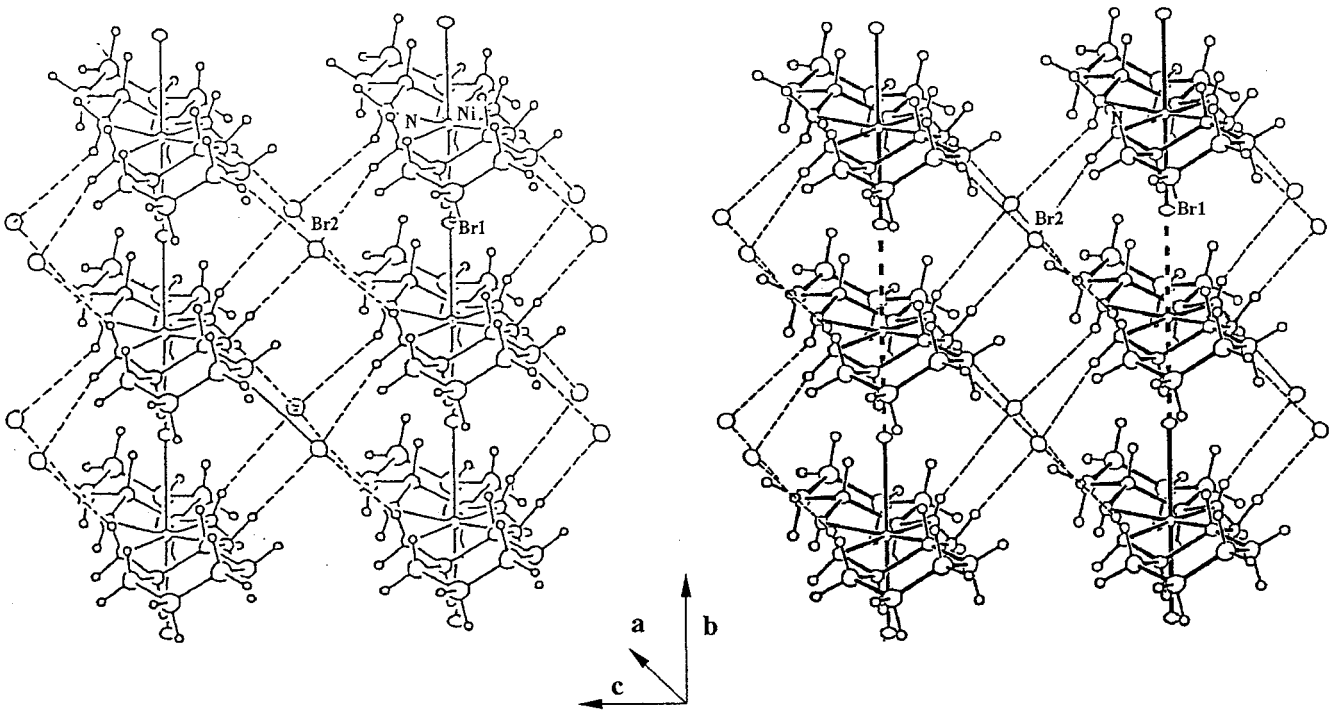

Figure 1. Structures of $[Ni(chxn)_2Br]Br_2$ (left) and $[Pd(chxn)_2][Pd(chxn)_2Br_2]Br_4$ (right).

of the scattered radiation was by a cooled photometrics CC 200 CCD camera system with operating temperature 153 K. Laser power at the crystals was held to <1 mW to avoid laser damage to samples. Wavenumber calibration was effected by reference to the Raman spectrum of indene or the emission spectrum of a Ne lamp.

The measurements of the XP and Auger spectra were performed using a ESCALAB MK II (VG Scientific Co.) photoelectron spectrometer with Mg Kα ($h\nu = 1253.6$ eV) or Al Kα ($h\nu = 1486.6$ eV) as an excitation light source at room temperature and 165 K. The base pressure of the analysis chamber was in the 10^{-10} Torr range. The excitation light was operated at low power (about 10 kV, 4 mA), because the samples degraded on prolonged exposure at high incident power. The Fermi level of the sample was determined by referring to that of a silver sample.

ESR spectra of single crystals and polycrystalline samples were measured on a JEOL JES-RE3X. The spin susceptibility was obtained by integrating twice the first-derivative ESR signal. The absolute magnitudes of the susceptibility and *g* values were calibrated using crystals of $CuSO_4 \cdot 5H_2O$ and DPPH as a standard, respectively.

For the measurements of the polarized reflectance spectra, a halogen−tungsten incandescent lamp was used. Light from the lamp was used by a concave mirror on the entrance slit of a 25 cm grating monochromator (JASCO CD 25). The monochromatic light from the exit slit was passed through a polarizer, and was focused on the specific surface of a single-crystal sample by using an optical microscope. Reflected light from the sample was focused by a concave mirror on the detector (a PdS cell or a photomultiplier tube). The optical conductivity spectra were obtained by using Kramers−Kronig transformation of the polarized reflectance spectra. The noise signals below 0.5 eV might be attributable to the ν(N−H) between the amino hydrogens and counter Br^- ions. The weak and strange feature appearing at around 1 eV in all spectra might be just an artifact related to the extrapolation in the case of Kramers−Kronig transformation.

Results and Discussion

We tried to determine the correct single-crystal structures of these Ni−Pd mixed-metal compounds, but we got only their averaged structures. Therefore, we obtained the crystal parameters such as the *a*, *b*, and *c* axes by using X-ray powder patterns. Figure 1 (left) shows the structure of $[Ni(chxn)_2Br]Br_2$, where the bridging Br^- ions are located at midpoints between two neighboring Ni ions, while Figure 1 (right) shows the structure of $Pd(chxn)_2Br_3$, where the bridging Br^- ions are distorted from midpoints between two neighboring Pd ions. Both compounds are isomorphous to each other (space group *I*222), although the positions of the bridging Br^- ions are different from each other. Both compounds have strong two-dimensional hydrogen bond networks. The crystal structures of $Ni_{1-x}Pd_x(chxn)_2Br_3$ are also found to be isomorphous (space group *I*222) with $[Ni^{III}(chxn)_2Br]Br_2$ and $Pd(chxn)_2Br_3$, although the positions of the bridging halogens are assumed to be different among these compounds. Accordingly, their structures are assumed as follows: The four N atoms of two chxn ligands are coordinated to Ni and Pd atoms in a planar fashion. The $M(chxn)_2$ moieties, lying on special position 222, are bridged by bromine atoms and stacked along the *b* axis, constructing linear chain structures. The neighboring $M(chxn)_2$ moieties along the chain are linked by the hydrogen bonds between amino hydrogens and counteranions. Moreover, there are the hydrogen bonds among the neighboring chains, constructing two-dimensional hydrogen bond networks parallel to the *bc* plane. The M−M distances are aligned along the *b* axis, which are lengthened with the increase of the Pd components due to the larger ionic radius of a Pd ion, compared with that of a Ni ion. On the other hand, the length of the *c* axis which corresponds to the interchain direction gradually decreases with the increase of the Pd ratios, since the counter Br^- ions can approach the chain (Figure 2). Such a negative correlation is also observed in $[M^{II}(chxn)_2][M^{IV}(chxn)_2X_2]Y_4$ (M = Pt and Pd; X = Cl, Br, and I; Y = ClO_4 and X).[2dh]

In the optical conductivity spectra, $[Ni^{III}(chxn)_2Br]Br_2$ shows the prominent absorption at 1.0 eV, which is attributable to the transition from the bridging Br^- to the upper Hubbard band of the Ni $3d_{z^2}$ orbitals along the chain, because the Ni^{III} compound takes the charge-transfer insulator.[8d] On the other hand, $[Pd^{II}(chxn)_2][Pd^{IV}(chxn)_2Br_2]Br_4$ shows the charge-transfer band at 0.5 eV, which is attributable to the intervalence transition from Pd^{II} d_{z^2} to Pd^{IV} d_{z^2} along the chain. In $Ni_{1-x}Pd_x(chxn)_2Br_3$, the spectra are not composed of the superposition of these two absoprtions but the single absorptions in the energy regions from

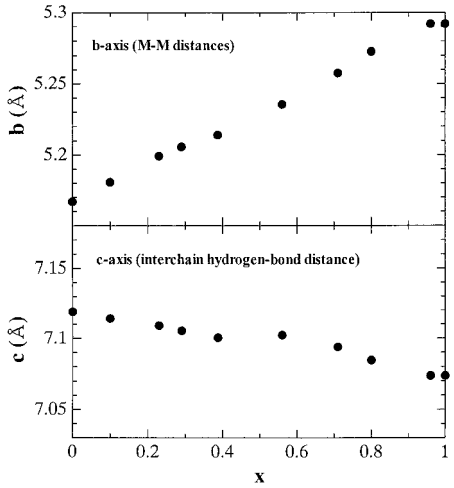

Figure 2. *b* and *c* axes of $Ni_{1-x}Pd_x(chxn)_2Br_3$.

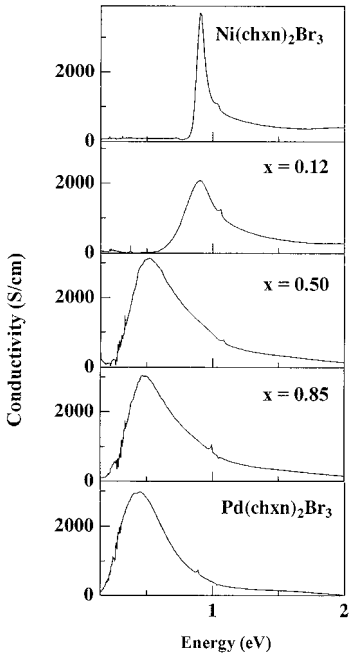

Figure 3. Optical conductivity spectra of the single crystals of $Ni_{1-x}Pd_x(chxn)_2Br_3$.

0.5 to 1.0 eV (Figure 3). Therefore, the new ground states are considered to be created in $Ni_{1-x}Pd_x(chxn)_2Br_3$.

In this system, the ν(N−H) signals around 3000 cm^{-1} in IR spectra are very good probes for evaluating their oxidation states.[10] $[Ni(chxn)_2Br]Br_2$ shows a singlet ν(N−H) signal around 3000 cm^{-1} due to the oxidation state of Ni^{III}, while $Pd(chxn)_2Br_3$ shows doublet ν(N−H) signals due to the oxidation states of Pd^{II} and Pd^{IV}. Figure 4 shows the IR spectra of $Ni_{1-x}Pd_x(chxn)_2Br_3$ at 12 K. The compounds with *x* larger than ca. 0.3 show the triplet signals which are assignable to the superposition of the doublet of the $Pd^{II}-Pd^{IV}$ state and the singlet of the Ni^{III} state. Therefore, the spectra may be divided into the singlet ν(N−H) of the Ni^{III} components and the doublet ν(N−H) of the $Pd^{II}-Pd^{IV}$ components. The divided peak energies are plotted in Figure 5. The peak energies of the Ni^{III} components are almost constant, while the peak energies of the Pd^{II} and Pd^{IV} components approach each other with an increase of the Ni^{III} components. This indicates that in this system the oxidation states of $Pd^{II}-Pd^{IV}$ mixed-valence states approach the Pd^{III} states with an increase of the Ni^{III} components.

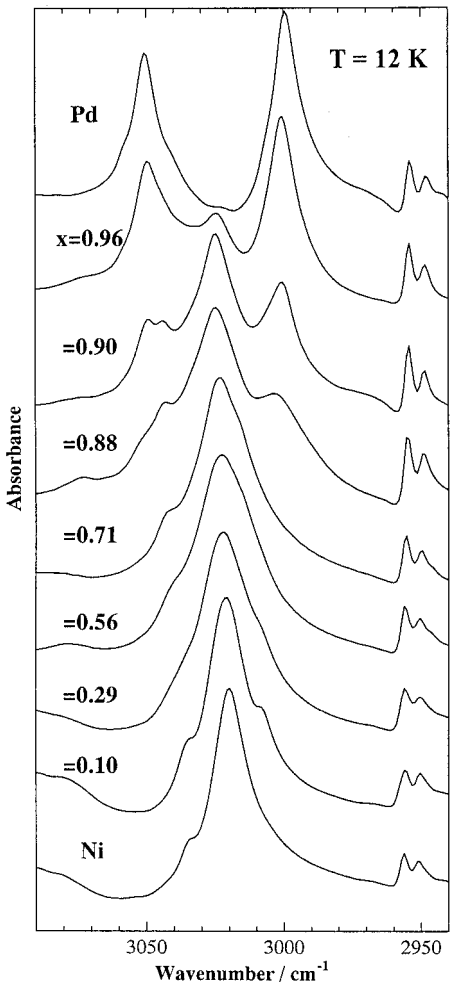

Figure 4. IR spectra of $Ni_{1-x}Pd_x(chxn)_2Br_3$ at 12 K.

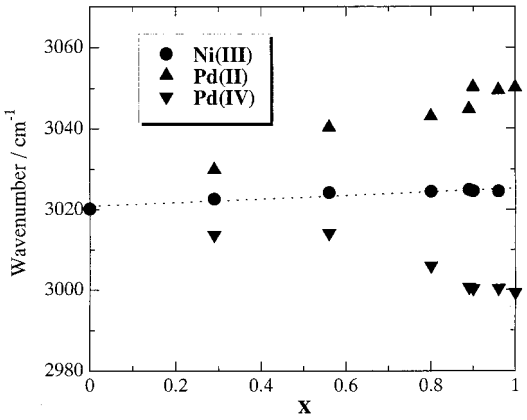

Figure 5. Peak energies of ν(N−H) of Ni^{III} species and $Pd^{II}-Pd^{IV}$ species.

Resonance Raman spectroscopy is another good probe for evaluating their oxidation states.[2b,c,f] So far, Clark's, Swanson's, and Papavassiliou's groups have measured resonance Raman spectra of many $M^{II}-M^{IV}$ mixed-valence compounds. The numbers and intensities of resonance Raman spectra depend on the oxidation states in these systems. Figure 6 shows their single-crystal Raman spectra of the Ni−Pd mixed-metal compounds along with those of the pure Ni^{III} and pure $Pd^{II}-Pd^{IV}$ mixed-valence compounds. The pure $Pd^{II}-Pd^{IV}$ mixed-valence com-

(10) Okaniwa, K.; Okamoto, H.; Mitani, T.; Toriumi, K.; Yamashita, M. *J. Phys. Soc. Jpn.* **1991**, *60*, 997.

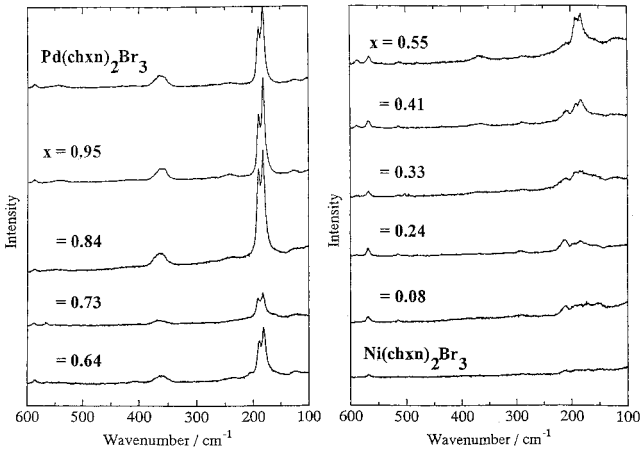

Figure 6. Single-crystal Raman spectra of $Ni_{1-x}Pd_x(chxn)_2Br_3$.

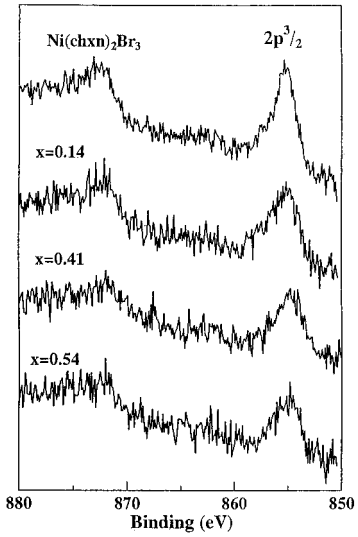

Figure 7. XP spectra of Ni 2p of $Ni_{1-x}Pd_x(chxn)_2Br_3$.

pound $Pd(chxn)_2Br_3$ shows characteristic progression of overtones of $\nu(Pd^{IV}-Br)$ in the resonance Raman spectrum, where the doublet peaks of $\nu(Pd^{IV}-Br)$ may be due to the isotope effect of the bridging Br^- ions. On the other hand, the pure Ni^{III} compound $[Ni(chxn)_2Br]Br_2$ shows no Raman spectrum because of the central positions of bridging Br^- ions between two neighboring Ni^{III} atoms. The numbers and intensities of the Raman spectra gradually decrease as *x* decreases. These results indicate that the positions of the bridging Br^- ions are gradually shifted to the central positions from the distorted positions with the increase of the Ni^{III} components. These results indicate that the oxidation states of the $Pd^{II}-Pd^{IV}$ mixed-valence states approach the Pd^{III} states with the increase of the Ni^{III} components. The results are consistent with those of IR spectra.

To directly investigate their oxidation states, the XP and Auger spectra were measured for these compounds at 165 K. Previously we measured the XP spectra of $[Pt(en)_2][Pt(en)_2X_2](ClO_4)_4$ (X = Cl, Br, and I). Going from Cl to I as the bridging halogens in these compounds, the differences of binding energies between Pt^{II} and Pt^{IV} components are gradually smaller; that is, their oxidation states approach the Pt^{III} states, because the electron−phonon interactions are weakened in this order.[11] Figure 7 shows that the XP spectra of the Ni $2p_{3/2}$ and Ni $2p_{1/2}$ in the Ni components of the Ni−Pd mixed-metal compounds

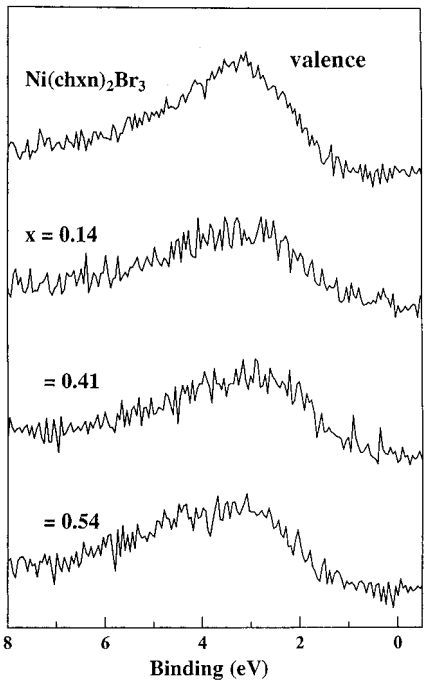

Figure 8. Valence-band XP spectra of Ni in $Ni_{1-x}Pd_x(chxn)_2Br_3$.

are essentially the same in these compounds, indicating that the oxidation states of Ni ions in all these compounds are +3. Figure 8 shows the valence-band XP spectra of the Ni components, which were obtained using Mg Kα radiation. In the spectra, broad peaks centered at 3−4 eV binding energies are observed. Both Ni 3d and bridging 3p (Cl) or 4p (Br) electrons will contribute to the XPS intensities in this region. Since the XPS cross section of the Ni 3d electrons is comparatively larger than those of Cl 3p and Br 4p electrons for Mg Kα radiation, the broad peak at 3−4 eV can be considered to have a dominantly 3d character. To evaluate the electron−electron correlation between 3d electrons (*U*), the Ni LVV Auger spectra were measured. Figure 9 shows the Auger spectra which were obtained by Al Kα radiation, since the strong N 1s XP line appears in the Auger spectral region with the excitation of the Mg Kα radiation. From these results, the *U* values are estimated to be 4−5 eV by using the equations as previously described.[8d] On the other hand, the XP spectra of the Pd $3d_{5/2}$ and Pd $3d_{3/2}$ in the Pd components of the Ni−Pd mixed-metal compounds change gradually from relatively broad to sharp shapes. Therefore, the spectra are resolved into the Pd^{II} and Pd^{IV} species as shown in Figure 10, where the Pd^{II} and Pd^{IV} species gradually approach each other with a decrease of the Pd components. As shown in Figure 11, the differences of the binding energies between Pd^{II} and Pd^{IV} components in these compounds gradually decrease with the increase of the Ni^{III} components, indicating that the oxidation states of $Pd^{II}-Pd^{IV}$ mixed-valence states gradually approach the Pd^{III} state. These results are consistent with those of the IR and Raman spectra. These results show that the electron−phonon interactions in $Pd^{II}-Pd^{IV}$ mixed-valence states are weakened with the increase of the Ni^{III} components which have strong electron correlations. Generally the electron−phonon interaction of the $Pd^{II}-Pd^{IV}$ mixed-valence state is estimated to be about 1 eV. Accordingly, the experimental results are very consistent with such values of the physical parameters. Previously, Okamoto et al. have estimated the magnitude of the electron correlation of the pure Ni^{III} compounds $[Ni^{III}(chxn)_2X]X_2$ to be 5−6 eV by using the XPS and Auger spectra.[8d] These values are about 1 eV larger than

(11) Yamashita, M.; Matsumoto, N.; Kida, S. *Inorg. Chim. Acta* **1978**, *31*, 381.

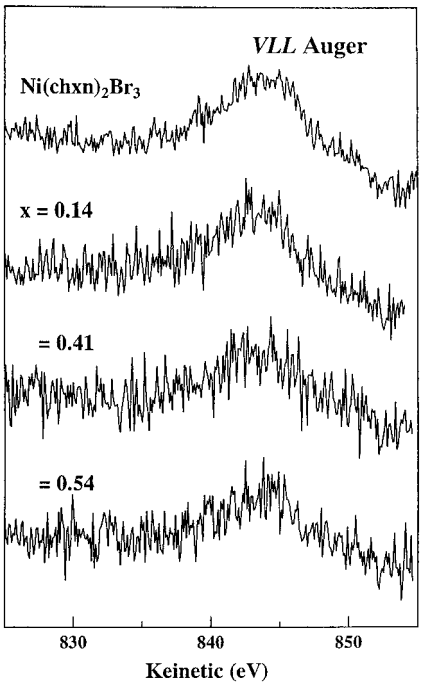

Figure 9. Ni LVV Auger spectra of $Ni_{1-x}Pd_x(chxn)_2Br_3$.

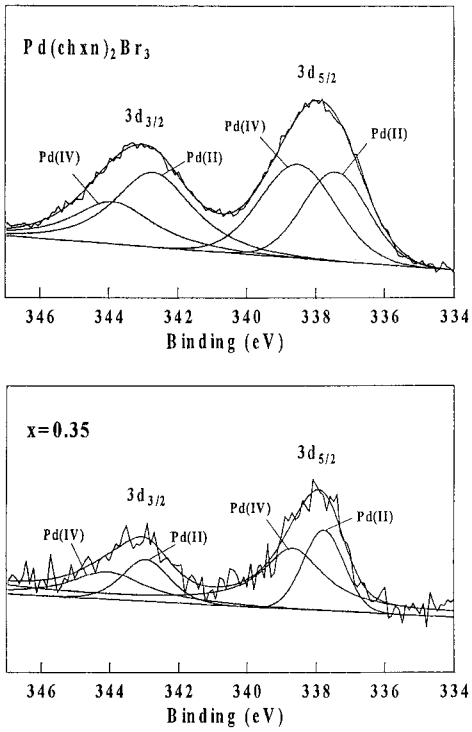

Figure 10. XP spectra of Pd 3d of $Ni_{1-x}Pd_x(chxn)_2Br_3$ and their resolution into the Pd^{II} and Pd^{IV} components.

those of the Ni−Pd mixed-metal compounds. Such results are well understood as a result of the competition between the electron correlation and electron−phonon interaction in these compounds.

To investigate the magnetic properties of these compounds, ESR spectra were measured by using the single-crystal (Figure 12) and polycrystalline samples. In the ESR spectra at room temperature, the pure Ni compound shows a very broad signal around $g = 2$, which is due to the very strong antiferromagnetic interaction among spins located on Ni $3d_{z^2}$ orbitals. The signals become gradually sharpened with the increase of the Pd

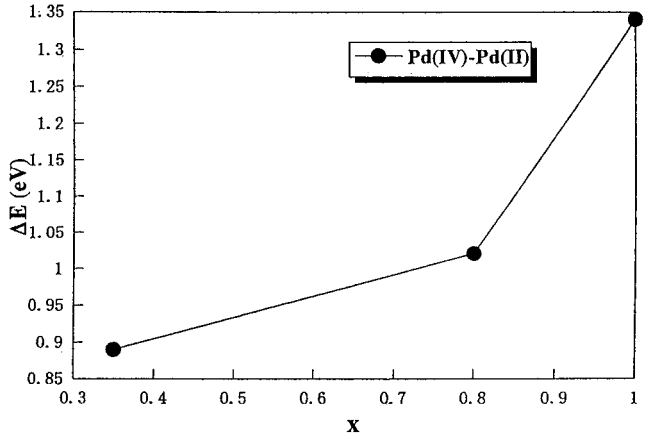

Figure 11. Difference of binding energies between Pd^{II} and Pd^{IV} components in $Ni_{1-x}Pd_x(chxn)_2Br_3$.

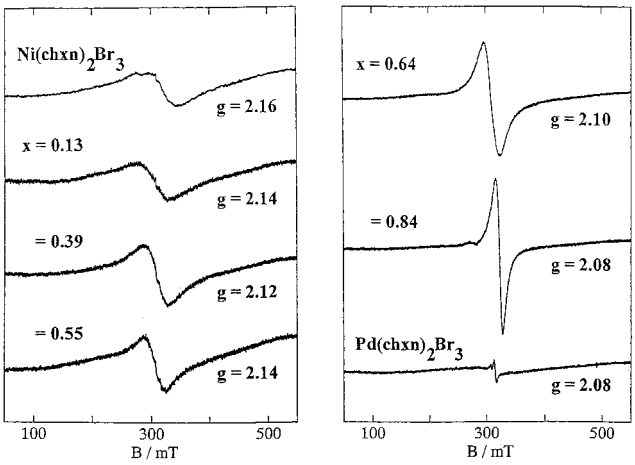

Figure 12. Single-crystal ESR spectra of $Ni_{1-x}Pd_x(chxn)_2Br_3$ at room temperature.

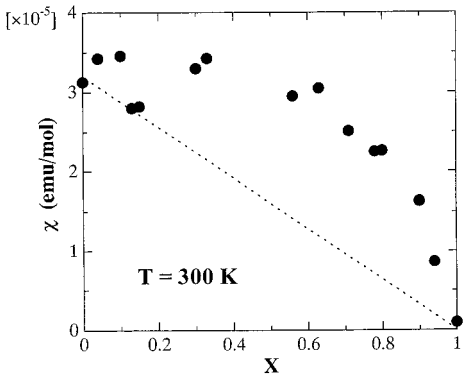

Figure 13. Spin susceptibilities of $Ni_{1-x}Pd_x(chxn)_2Br_3$ at room temperature. The dotted line shows the linear summation of magnetic Ni^{III} and nonmagnetic Pd.

components due to the spin−lattice interaction.[8c] The spin susceptibilities at room temperature are plotted in Figure 13.[12] In Figure 13, the dotted line shows the linear summation of the pure Ni^{III} and nonmagnetic Pd^{II}−Pd^{IV} constituents. The spin susceptibilities obtained experimentally are not linear but deviated to the upper sites. That is, the spin susceptibilities are increased in the Ni−Pd mixed-metal compounds. There are two

(12) (a) Kuroda, S.; Marumoto, K.; Manabe, T.; Yamashita, M. *Synth. Met.* **1999**, *103*, 2155. (b) Marumoto, K.; Kuroda, S.; Manabe, T.; Yamashita, M. *Synth. Met.* in press. (c) Marumoto, K.; Tanaka, H.; Kuroda, S.; Manabe, T.; Yamashita, M. *Phys. Rev. B.* **1999**, *60*, 7699.

possibilities for the enhancement of the spin susceptibilities: (1) the $Pd^{II}-Pd^{IV}$ components changing to the magnetic Pd^{III} components, (2) the cutting effect of the antiferromagnets with nonmagnetic components.[13] In the latter case, the Curie impurities should increase; however, such phenomena were not observed. Therefore, reasonably the $Pd^{II}-Pd^{IV}$ states change into Pd^{III} states with the increase of the Ni^{III} components. Such a result is consistent with those of the IR, Raman, and XPS spectra.

According to the recent theoretical study by Iwano, such a conversion from CDW to SDW in Pd sites may be caused by the effect that the Hubbard *U* at Ni sites is larger compared with the electron−phonon interaction. The effect of the random mixing of Ni and Pd in a one-dimensional chain was treated by using a Peierls−Hubbard model and a mean-field approximation. The theoretical results have shown that the 50% concentration of Ni sites is enough to destroy the order of CDW, which is consistent with the present experimental results.[14]

More detailed investigations are now in progress.

(13) (a) Tonegawa, T.; Shiba, H.; Pincus, P. *Phys. Rev. B.* **1975**, *11*, 4683. (b) Tonegawa, T. *Phys. Rev. B* **1976**, *14*, 3166.
(14) Iwano, K. *J. Phys. Soc. Jpn.* **1999**, *68*, 935.

Conclusion

We have obtained single-crystals of the Ni−Pd mixed-metal compounds $Ni_{1-x}Pd_x(chxn)_2Br_3$, where the electron correlation in Ni^{III} states (SDW) and the electron−phonon interaction in $Pd^{II}-Pd^{IV}$ mixed-valence states (CDW) compete with each other. As a result, the $Pd^{II}-Pd^{IV}$ mixed-valence states gradually approach the Pd^{III} state with the decrease of the Pd ratios influenced by the increase of the Ni^{III} states. This means that the electron−phonon interactions in the $Pd^{II}-Pd^{IV}$ mixed-valence states are weakened by the strong electron correlation in the Ni^{III} states. In other words, the charge density wave strengths of Pd sites can be tuned by competition between the electron−phonon interaction of the $Pd^{II}-Pd^{IV}$ states and the electron correlation of the Ni^{III} states in the Ni−Pd mixed-metal compounds $Ni_{1-x}Pd_x(chxn)_2Br_3$.

Acknowledgment. This work was partly supported by The Mazda Foundation's Research Grant, and a Grant-in-Aid for Scientific Research on Priority Areas ("Metal-assembled Complexes") from the Ministry of the Education, Science and Culture of Japan.

IC990219I